JOC Article

Synthesis, Structures, and Properties of Disubstituted Heteroacenes on One Side Containing Both Pyrrole and Thiophene Rings

Ting Qi,[†] Wenfeng Qiu,[‡] Yunqi Liu,*[,‡] Hengjun Zhang,[†] Xike Gao,[†] Ying Liu,[†] Kun Lu,[†] Chunyan Du,[†] Gui Yu,[‡] and Daoben Zhu[‡]

Graduate School of Chinese Academy of Sciences, Beijing 100190, China; Beijing National Laboratory for Molecular Sciences, Organic Solids Laboratory, Institute of Chemistry, Chinese Academy of Sciences, Beijing 100190, China

liuyq@mail.iccas.ac.cn

Received March 20, 2008

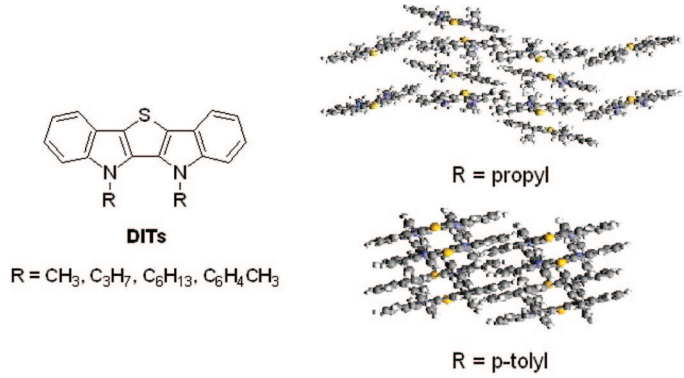

A new series of ladder-type heteroacenes containing both pyrrole and furan rings, 5,6-disubstituted diindolo[3,2-*b*:4,5-*b*′]thiophenes (DITs), were effectively synthesized from N-functionalized 3,3′-dibromo-2,2′-biindoles undergoing intramolecular cyclization with bis(phenylsulfonyl) sulfide and organolithium. Single-crystal X-ray results demonstrate that 5,6-dipropyldiindolo[3,2-*b*:4,5-*b*′]thiophene (**4b**) forms a herringbone-type of packing motif and 5,6-di(*p*-tolyl)diindolo[3,2-*b*:4,5-*b*′]thiophene (**4d**) forms a parallel packing motif. Both of them have S−S contacts, enhancing the electronic transport between molecules. Their photophysical properties suggest that the skeleton of diindolo[3,2-*b*:4,5-*b*′]thiophene is more favorable to aggregate in solid than that of indolo[3,2-*b*]carbazole. The large band gaps and low-lying HOMO energy levels could result in much better stability.

Introduction

The design and synthesis of new π-conjugated organic semiconductors are attracting more and more attention due to their potential applications for various optoelectronic devices.[1] In particular, the linearly fused acenes have applications in organic field-effect transistors (OFETs), light emitting diodes (LEDs), and photovoltaic cells.[2] Recent research interest has primarily focused on pentacene and its derivatives, in which pentacene exhibits outstanding charge carrier mobility of 1.5 $cm^2\ V^{-1}\ s^{-1}$ for OFETs (on chemically modified SiO_2/Si substrate).[3] However, pentacene has some shortcomings when applied in devices, such as poor solubility, limited stability in ambient conditions,[4] and unfavorable stacking in the solid state.[5]

One strategy to overcome these shortcomings is to introduce heteroatoms in the fused-ring system to construct more stable ladder-type fused molecules. New π-extended pentacene-like heteroacenes, e.g., 5,7,12,14-tetraazapentacene,[6] indole[3,2-*b*]carbazole,[7] pentathieoacene,[8] anthradithiophene,[9] benzo[1,2-*b*:4,5-*b*′]bis[*b*]benzothiophene,[10] tetraceno[2,3-*b*]thiophene,[11]

[†] Graduate School of Chinese Academy of Sciences.
[‡] Chinese Academy of Sciences.

(1) Dimitrakopoulos, C. D.; Malenfant, P. R. L. *Adv. Mater.* **2002**, *14*, 99.
(2) (a) Anthony, J. E. *Chem. Rev.* **2006**, *106*, 5028. (b) Sun, Y.; Liu, Y.; Zhu, D. *J. Mater. Chem.* **2005**, *15*, 53.
(3) (a) Lin, Y.-Y.; Gundlach, D. J.; Nelson, S. F.; Jackson, T. N. *IEEE Electron Device Lett.* **1997**, *18*, 606. (b) Nelson, S. F.; Lin, Y.-Y.; Gundlach, D. J.; Jackson, T. N. *Appl. Phys. Lett.* **1998**, *72*, 1854.
(4) Weidkamp, K. P.; Afzali, A.; Tromp, R. M.; Hamers, R. J. *J. Am. Chem. Soc.* **2004**, *126*, 12740.
(5) (a) Anthony, J. E.; Eaton, D. L.; Parkin, S. R. *Org. Lett.* **2002**, *4*, 15. (b) Sheraw, C. D.; Jackson, T. N.; Eaton, D. L.; Anthony, J. E. *Adv. Mater.* **2003**, *15*, 2009.

10.1021/jo800622y CCC: $40.75
Published on Web 05/22/2008

and dibenzo[*d*,*d*′]thieno[3,2-*b*:4,5-*b*′]dithiophene,[12] have been developed and tested as active semiconducting channels in OFETs. We found that the reported molecules mainly introduced sulfur or nitrogen as bridging atoms. To the best of our knowledge, the introduction of sulfur and nitrogen together in the pentacene-like system as OFET materials has still not been reported. The incorporation of sulfur as thiophene substructure would exhibit a variety of intra- and intermolecular interactions, such as van der Waals interactions, $\pi-\pi$ stacking, and sulfur−sulfur interactions, essential to achieve high charge mobility.[13] Furthermore, Ong et al. recently reported that 5,11-disubstituted indolo[3,2-*b*]carbazole displayed the high mobility of 0.12 $cm^2\ V^{-1}\ s^{-1}$ and good environmental stability, and the introduction of nitrogen atoms can well increase the stability of materials.[7b] In addition, the research on crystal structure of organic semiconductors is very important to explore structure−property relationships. Notably, substituents can affect molecular solid-state order.[9a,14] At present, we found that the substituents of the linearly fused acenes studied mainly lie in one or two terminals of molecular backbone or two sides of molecular central rings. However, the crystal packing about the substituents of acenes on one side of central rings is rarely studied. Recently, only the groups of Bao,[15] Nuckolls,[16] and Nakano[17] studied crystal packing of monosubstituted acenes on one side, respectively. This paper will focus on disubstituted crystal packing of acenes on one side needed for complementary study of structure−property relationships.

In this work, we designed and synthesized a new series of ladder-type pentacene-like heteroacenes **4a**−**d** containing pyrrole and thiophene rings, diindolo[3,2-*b*:4,5-*b*′]thiophene (DIT), motivated by aforementioned characteristics. The reaction of bis(phenylsulfonyl)sulfide with 3,3′-dilithiodiaryl generated from biaryl bromide has been a common method for the preparation of dithieno[3,2-*b*:2′,3′-*d*]thiophene.[18] We envisioned that sulfur-bridged N-functionalized 2,2′-biindole could be synthesized in a similar way by the reaction of bis(phenylsulfonyl)sulfide with N-functionalized 3,3′-dilithio-2,2′-biindole (Scheme 1). The lithium−halogen exchange reaction of bromoindole with organolithium conveniently produces aryllithiums,[19] and 3,3′-dibromo-2,2′-biindole is easily available by bromination of 2,2′-biindole directly. Thus, these reactions enable us to design an efficient synthetic route to different substituent ladder-type heteroacenes. Different substituents for structural modification may not only improve the solubility and the thin film packing, but also exert subtle influences on the molecular physical properties. Structural and physical properties of the synthesized heteroacenes are discussed.

SCHEME 1

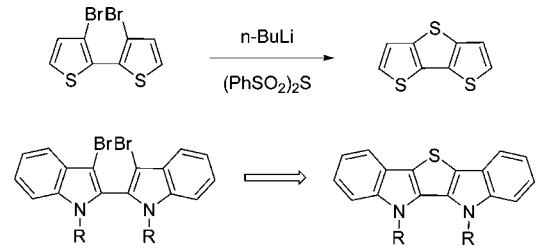

Results and Discussion

Synthesis. The synthetic route to DITs **4a**−**d** is outlined in Scheme 2. We used N-functionalized indole as the starting material, because the substituents can not only improve the solubility of compounds, but also make compounds subjected to the lithiation in the next steps. Four substituents were selected, and alkyl (propyl[20] and hexyl[20]) and aryl (*p*-tolyl[21]) were introduced under different reaction conditions, respectively, according to the literature. Indole easily reacted with various alkyl bromides in the presence of KOH to give N-alkyl-substituted products **1b** and **1c**. The aryl group was introduced onto the indole nitrogen by treating indole with aryl iodide in the presence of potassium carbonate and CuO to give N-aryl-substituted product **1d**. N-Functionalized indoles (**1a**−**d**) were then reacted with *n*-butyllithium at reflux and oxidized by $CuCl_2$ to produce symmetric 2,2′-coupling dimers **2a**, **2b**, **2c**, and **2d** in moderate yields.[22] Bromination of **2a**−**d** (bromine, DMF) gave rise to 3,3′-dibromo-2,2′-biindole (**3a**−**d**) in high yield directly.[23] The final ring closure reaction succeeded by using bis(phenylsulfonyl) sulfide in generating the appropriate anions during the lithiation to give the target products **4a**, **4b**, **4c**, and **4d** in 51%, 53%, 56%, and 55% yields, respectively. As expected, the solubility of N-alkylated compounds (**4a**−**c**) increases with the lengthening alkyl chains. Overall, all of these new compounds exhibit good solubility in common solvents such as $CHCl_3$, CH_2Cl_2, THF, toluene, and chlorobenzene, thus enabling purification by column chromatography.

Crystal Packing Studies: X-ray Analyses of DITs 4b and 4d. Most studies indicate that the linearly fused acenes

(6) Ma, Y.; Sun, Y.; Liu, Y.; Gao, J.; Chen, S.; Sun, X.; Qiu, W.; Yu, G.; Cui, G.; Hu, W.; Zhu, D. *J. Mater. Chem.* **2005**, *15*, 4894.
(7) (a) Li, Y. N.; Wu, Y. L.; Gardner, S.; Ong, B. S. *Adv. Mater.* **2005**, *17*, 849. (b) Wu, Y.; Li, Y.; Gardner, S.; Ong, B. S. *J. Am. Chem. Soc.* **2005**, *127*, 614. (c) Wakim, S.; Bouchard, J.; Simard, M.; Drolet, N.; Tao, Y.; Leclerc, M. *Chem. Mater.* **2004**, *16*, 4386.
(8) Xiao, K.; Liu, Y.; Qi, T.; Zhang, W.; Wang, F.; Gao, J.; Qiu, W.; Ma, Y.; Cui, G.; Chen, S.; Zhan, X.; Yu, G.; Qin, J.; Hu, W.; Zhu, D. *J. Am. Chem. Soc.* **2005**, *127*, 13281.
(9) (a) Payne, M. M.; Parkin, S. R.; Anthony, J. E.; Kuo, C.-C.; Jackson, T. N. *J. Am. Chem. Soc.* **2005**, *127*, 4986. (b) Laquindanum, J. G.; Katz, H. E.; Lovinger, A. J. *J. Am. Chem. Soc.* **1998**, *120*, 664.
(10) Ebata, H.; Miyazaki, E.; Yamamoto, T.; Takimiya, K. *Org. Lett.* **2007**, *9*, 4499.
(11) (a) Valiyev, F.; Hu, W. S.; Chen, H. Y.; Kuo, M. Y.; Chao, I.; Tao, Y. T. *Chem. Mater.* **2007**, *19*, 3018. (b) Tang, M. L.; Okamoto, T.; Bao, Z. N. *J. Am. Chem. Soc.* **2006**, *128*, 16002.
(12) Gao, J.; Li, R.; Li, L.; Meng, Q.; Jiang, H.; Li, H.; Hu, W. *Adv. Mater.* **2007**, *19*, 3008.
(13) (a) Coropceanu, V.; Cornil, J.; da Silva Filho, D. A.; Olivier, Y.; Silbey, R.; Brédas, J.-L. *Chem. Rev.* **2007**, *107*, 926. (b) Lemaur, V.; da Silva Filho, D. A.; Coropceanu, V.; Lehmann, M.; Geerts, Y.; Piris, J.; Debije, M. G.; van de Craats, A. M.; Senthilkumar, K.; Siebbeles, L. D. A.; Warman, J. M.; Brédas, J.-L.; Cornil, J. *J. Am. Chem. Soc.* **2004**, *126*, 3271. (c) Marseglia, E. A.; Grepioni, F.; Tedesco, E.; Braga, D. *Mol. Cryst. Liq. Cryst.* **2000**, *348*, 137. (d) Barbarella, G.; Zambianchi, M.; Bongini, A.; Antolini, L. *Adv. Mater.* **1993**, *5*, 834.
(14) (a) Bénard, C. P.; Geng, Z.; Heuft, M. A.; VanCrey, K.; Fallis, A. G. *J. Org. Chem.* **2007**, *72*, 7229. (b) Takahashi, T.; Li, S.; Huang, W.; Kong, F.; Nakajima, K.; Shen, B.; Ohe, T.; Kanno, K. *J. Org. Chem.* **2006**, *71*, 7967.
(15) Moon, H.; Zeis, R.; Borkent, E.-J.; Besnard, C.; Lovinger, A. J.; Siegrist, T.; Kloc, C.; Bao, Z. *J. Am. Chem. Soc.* **2004**, *126*, 15322.
(16) Miao, Q.; Chi, X.; Xiao, S.; Zeis, R.; Lefenfeld, M.; Siegrist, T.; Steigerwald, M. L.; Nuckolls, C. *J. Am. Chem. Soc.* **2006**, *128*, 1340.
(17) Kawaguchi, K.; Nakano, K.; Nozaki, K. *Org. Lett.* **2008**, *10*, 1199.
(18) Allared, F.; Hellberg, J.; Remonen, T. *Tetrahedron Lett.* **2002**, *43*, 1553.
(19) Clayden, J. *Tetrahedron Organic Chemistry Series*, 1st ed.; Pergamon: Oxford, 2002; Vol. 23, Chapter 3.
(20) Gong, W.; Li, Q.; Li, Z.; Lu, C.; Zhu, J.; Li, S.; Yang, J.; Cui, Y.; Qin, J. *J. Phys. Chem. B* **2006**, *110*, 10241.
(21) Zhang, H.-C.; Derian, C. K.; McComsey, D. F.; White, K. B.; Ye, H.; Hecker, L. R.; Li, J.; Addo, M. F.; Croll, D.; Eckardt, A. J.; Smith, C. E.; Li, Q.; Cheung, W.-M.; Conway, B. R.; Emanuel, S.; Demarest, K. T.; Andrade-Gordon, P.; Damiano, B. P.; Maryanoff, B. E. *J. Med. Chem.* **2005**, *48*, 1725.
(22) (a) Bergman, J.; Eklund, N. *Tetrahedron* **1980**, *36*, 1439. (b) Pindur, U.; Kim, M.-H. *Tetrahedron* **1989**, *45*, 6427.
(23) (a) Pindur, U.; Kim, Y.-S.; Schollmeyer, D. *J. Heterocycl. Chem.* **1994**, *31*, 377. (b) Pindur, U.; Kim, Y. S.; Schollmeyer, D. *J. Heterocycl. Chem.* **1995**, *32*, 1335.

SCHEME 2. Synthesis of Compounds 4a−d

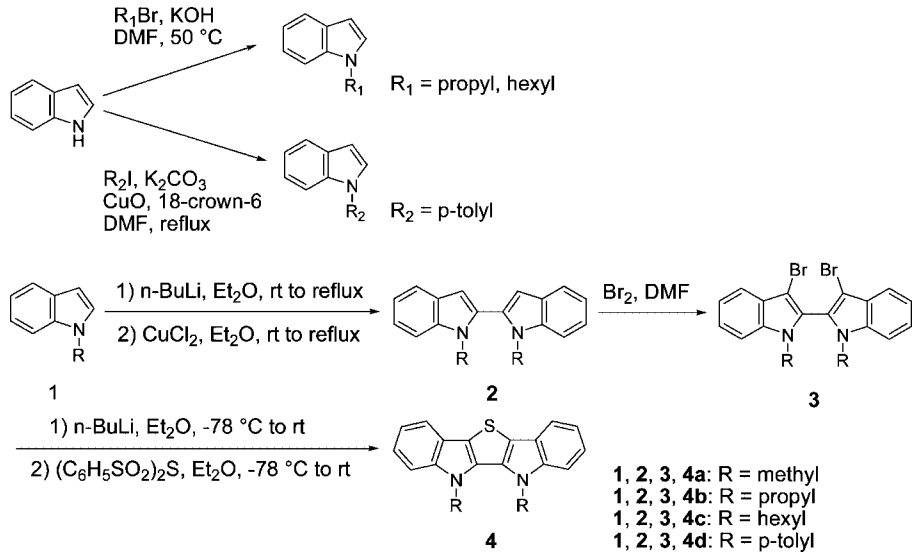

commonly adopt herringbone or parallel packing motif. We obtained colorless block single crystals of **4b** and **4d** by slow evaporation of hexane and vacuum sublimation, respectively. The detailed crystallographic data can be found in the Supporting Information. X-ray analyses display that the size of substituents has an effect on molecular solid-state packing.

The tolyl-substituted DIT **4d** prefers to pack in a parallel pattern (Figure 2). As shown in Figure 1, due to the steric hindrance that the tolyl groups impose, the molecules in a stack are alternately rotated by 180°. This similar anti conformation also exists in the **4b** crystal structure (Figure S1, Supporting Information). Possibly due to the DIT backbone having a molecular dipole moment, the orientation of molecules alternates between layersr to minimize the dipolar interactions.[24] Therefore, the interlayer adjacent two molecules form a dimer. The tolyl groups are inclined at approximately 70° with respect to the acene plane. Short C−H···π intermolecular interactions exist between pendant tolyl and the conjugated plane at 2.77 Å. Notably, this compound forms a face−face slipped π-stacking structure. The short C−C contacts (3.47 Å) exist in an edge-to-edge manner, shown with dashed lines in Figure 2. The distance between adjacent full overlapped molecules in the column is 9.83 Å (Figure S4, Supporting Information). Furthermore, intermolecular S−S (3.63 Å) and S···H (2.91 Å) interactions exist between columns consisting of dimers (Figure S6, Supporting Information).

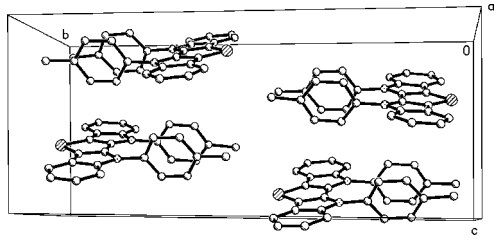

FIGURE 1. Crystal cell packing structure of **4d**, with hydrogen atoms removed for clarity.

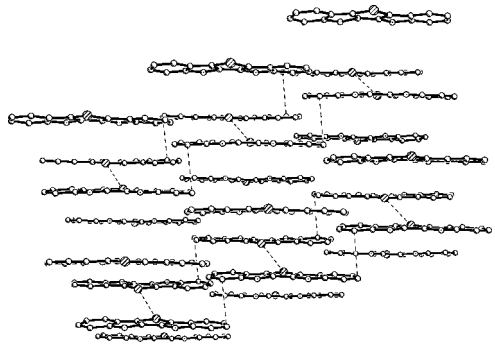

FIGURE 2. Crystal packing of **4d**, view down the *b*-axis, with hydrogen atoms and tolyl groups removed for clarity.

The propyl-substituted DIT **4b** prefers to pack in a herringbone pattern (Figure 3). However, different from commonly reported herringbone arrangement, the crystal packing structure of **4b** is more complicated. As shown in Figure 3, there are three independent molecular configurations in the crystal to construct three types of stacking columns arranged in an edge-to-face fashion. Therefore, three types of herringbone patterns are interlaced in the **4b** crystal structure. Similar to **4d**, due to the dipolar interactions, the interlayer adjacent two molecules also form a dimer, but they are interlaced because of alkyl cooperation (Figure S1, Supporting Information). The two adjacent molecules in a stacking column are rotated by almost 180° (column a and column b) and 157° (column c), respectively (Figure S2, Supporting Information). Short C−H···π (2.71 Å average) intermolecular interactions between pendant propyl and the conjugated plane and S−S (3.66 Å in columns a and c and 3.56 Å in column b) and S···H (3.00 Å average) contacts exist along the *c*-axis. Meanwhile, three kinds of herringbone packing patterns show three kinds of C−H···π interactions existing between adjacent edge-to-face molecules along the *a*-axis (at 2.74 Å between columns a and b, 3.07 Å between columns a and c, and 3.26 Å between columns b and c, respectively). The two types of herringbone arrangements with much longer C−H···π interactions show a trend to parallel packing, indicative of the transition from herringbone to parallel packing. The mean distance between adjacent mostly overlapped molecules in the column is 7.69 Å shorter than that of **4d** (9.83 Å), indicating that **4b** has a tighter packing structure because its

(24) (a) He, M.; Zhang, F. *J. Org. Chem.* **2007**, *72*, 442. (b) Miao, Q.; Lefenfeld, M.; Nguyen, T. Q.; Siegrist, T.; Kloc, C.; Nuckolls, C. *Adv. Mater.* **2005**, *17*, 407.

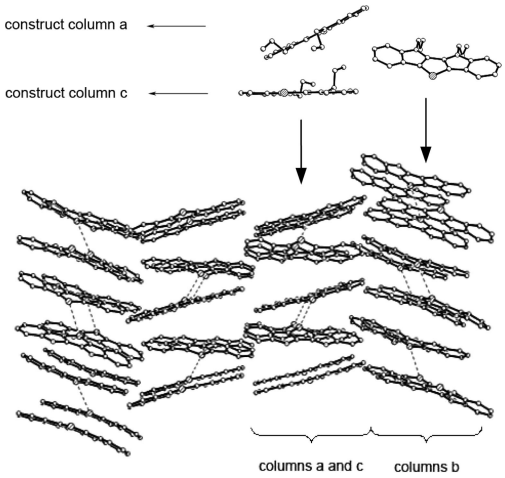

FIGURE 3. Crystal packing of **4b**, view down the *b*-axis, with hydrogen atoms and propyl groups removed for clarity (on the bottom).

TABLE 1. Photophysical Data of Compounds 4a−d and 5

	solution			film[d]		
compd	λ_{abs}[a] (nm)	λ_{lum}[b] (nm)	E_g[c] (eV)	λ_{abs} (nm)	λ_{lum}[b] (nm)	E_g[c] (eV)
4a	344, 353	370, 384	3.30	352, 370	397	3.25
4b	345, 353	372, 385	3.31	350, 370	393	3.14
4c	344, 353	372, 385	3.32	348, 366	391	3.18
4d	343, 351	371, 383	3.32	348, 364	401	3.16
5[e]	340, 388, 410			341, 415		2.8

[a] Measured in a dilute CH_2Cl_2 solution (2×10^{-5} M). [b] Excited at the absorption maxima. [c] Estimated from the onset of absorption ($E_g = 1240/\lambda_{onset}$). [d] Films were vacuum deposited (50 nm, quartz substrate). [e] From ref 7b.

steric hindrance of substituents is much smaller. We could predict that **4a** with the smallest substituents may have the tightest packing structure. Unfortunately, crystals of **4a** suitable for single-crystal analysis have not been obtained.

The substituents of this synthesized series are all on the same side of the central rings of molecular conjugated backbone. This particular position of substituents makes molecules have particular configurations, which form dimers more easily. Their crystal structures show that not only the size of the substituents but also the molecular dipole moment has a dramatic effect on the solid-state packing. Meanwhile, the S−S interactions enhance the electronic transport between molecules. Compared with the crystal structure of 5,11-diphenylindolo[3,2-*b*]carbazole, which has little overlap between π-planes of the fused-ring framework,[25] **4d** obviously bears enhanced π-stacking in the crystal lattice because of the incorporation of a thienyl group (Figure 2). The research would yield complementary and useful information to study structure−property relationships about OFET semiconductors.

Optical Properties. The photophysical properties of DITs **4a−d** are tabulated in Table 1, together with the data of 5,11-dimethylphenylindolo[3,2-*b*]carbazole (**5**) for comparison (Figure 4).

For this series of compounds, although the substituents are different, the variations of absorption and emission wavelengths in a dilute solution are much less pronounced. They all exhibit similar vibronic $\pi-\pi^*$ transition absorption bands with the longest maxima around 340−355 nm and emission bands with the maxima around 385 nm due to their identical skeletons (Figure 5), the diindolo[3,2-*b*:4,5-*b*′]thiophene unit. Shown in Figure 6 are the spectra of vacuum-deposited films of **4a−d** on quartz substrates. All compounds show sharp band edges suggesting little structural disorder. Compared with those in solution, broadening of the absorption spectrum and a 13−17 nm red-shift of all peaks in pristine film were observed because of the formation of the aggregates. Such a pronounced change of the absorption spectrum is a result of the delocalization of the exciton within a cofacial stack induced by the $\pi-\pi$ interaction, which was also evidenced by a related 6−18 nm red-shift of the photoluminescence spectrum shown in Table 1. It is worth noting that obvious absorbance enhancement of the onset peak relative to the second was observed in the alkyl-substituted compounds, and the relative intensity increased with the decreasing length of the alkyl chain. This is the result of intermolecular interactions, suggesting that the shorter the length of the alkyl chain, the more favorable $\pi-\pi$ stacking is. It is identical with the degree of relative red-shift of emission maxima from solution to films, in the order **4a** > **4b** > **4c**.

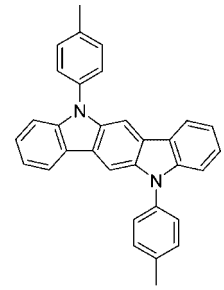

FIGURE 4. The molecular structure of 5,11-dimethylphenylindolo[3,2-*b*]carbazole (**5**).

The absorption spectrum of a dilute solution of **5** showed red-shift relative to **4d**. Their structural difference is the central fused benzene ring of the backbone for **5** changed to thiophene for **4d**, resulting in spectral change. Matzger et al. stated that adding the sulfur atom acts to widen the HOMO−LUMO gap induced by LUMO destabilization.[26] This could be the reason that **4d** displays a higher energy band compared to **5**. The absorption spectra of **4d** display a 13 nm red-shift from a dilute solution to a film, evidently larger than that of **5**, indicating that the skeleton of diindolo[3,2-*b*:4,5-*b*′]thiophene is more favorable to aggregate in solid than that of indolo[3,2-*b*]carbazole. The crystal structure of **4d** also confirmed this conclusion further. The optical band gaps estimated from the absorption edges of the thin-film spectra for **4a−d** are around 3.2 eV, larger than **5** (2.8 eV). Semiconductors with large band gaps, which absorb in the UV or near-UV regions, are suitable for fabricating transparent OTFT circuits used for optoelectronic devices requiring circuit transparency.[27]

Electrochemical Properties. Cyclic voltammetry of DITs **4a−d** showed a reversible oxidation wave (Figure 7). The oxidation peaks ($E^{1/2}$ values) of **4a**, **4b**, **4c**, and **4d** were found at +0.93, +0.94, +0.94, and +0.98 V vs Ag/AgCl, respectively. Given the ferrocene/ferrocenium (Fc/Fc^+) couple was used as the internal standard,[28] HOMO levels of **4a**, **4b**, **4c**, and **4d** were estimated by using oxidation onsets −5.29, −5.31, −5.29,

(25) Kawaguchi, K.; Nakano, K.; Nozaki, K. *J. Org. Chem.* **2007**, *72*, 5119.

(26) Zhang, X.; Matzger, A. J. *J. Org. Chem.* **2003**, *68*, 9813.

(27) Nomura, K.; Ohta, H.; Ueda, K.; Kamiya, T.; Hirano, M.; Hosono, H. *Science* **2003**, *300*, 1269.

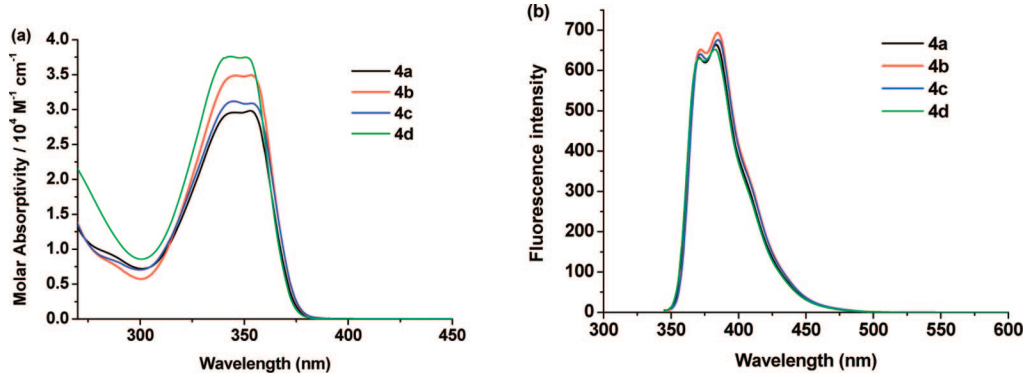

FIGURE 5. (a) Absorption and (b) emission spectra (2×10^{-5} M) of compounds **4a**−**d** in CH_2Cl_2.

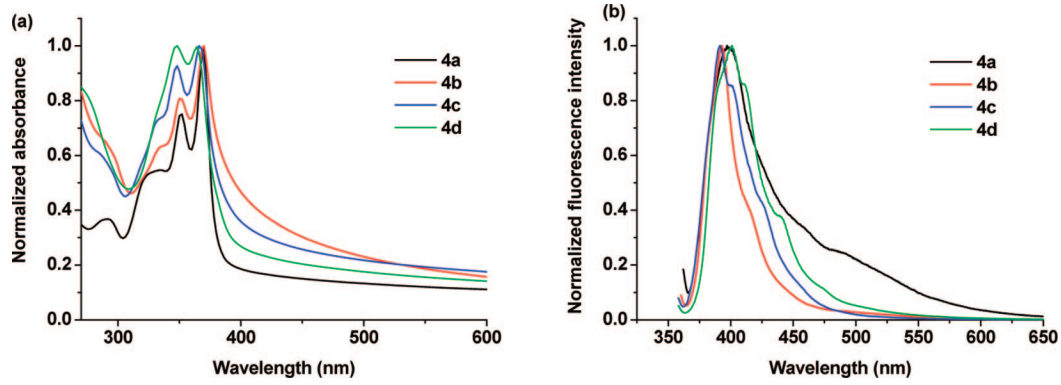

FIGURE 6. (a) Absorption and (b) emission spectra for films of compounds **4a**−**d** on the quartz substrate.

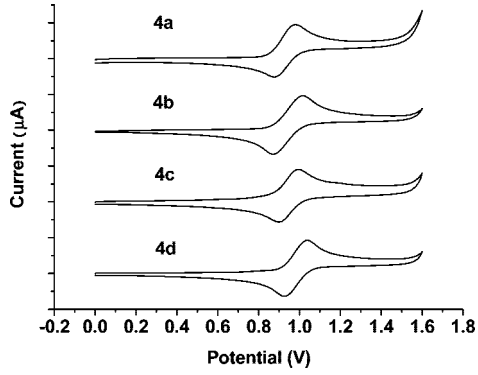

FIGURE 7. Cyclic voltammograms of **4a**−**d** ($c = 10^{-3}$ M) in CH_2Cl_2 containing Bu_4NPF_6 (0.01 M) as supporting electrolyte at room temperature, with a scan rate of 100 mV/s.

and −5.35 eV from vacuum, respectively. On the basis of the HOMO energy levels and the optical band gaps (E_g) evaluated from the onset wavelengths of UV−vis absorption spectra, LUMO energy levels were calculated (Table 2). In the produced heteroacenes, the introduction of different substituents has little influence on the HOMO and LUMO energy levels. However, it should be noted that **4d** has the relative highest oxidation peak potential and the lowest HOMO and LUMO energy levels, which can be attributed to sufficient resonance stabilization to injected hole carriers for aryl substitution. These presented compounds practically all have lower lying HOMO energy levels and larger band gaps than pentacene (E_{HOMO} = −4.60 eV, E_g = 2.21 eV),[29] which should indicate better stabilities against oxygen under ambient conditions.

TABLE 2. Cyclic Voltammogram Data and Optical Band Gaps of 4a−d

compd	$E^{1/2}{}_{ox}{}^a$ (V)	$E_{HOMO}{}^b$ (eV)	$E_{LOMO}{}^c$ (eV)	$E_g{}^d$ (eV)
4a	0.93	−5.29	−1.99	3.30
4b	0.94	−5.31	−2.00	3.31
4c	0.94	−5.29	−1.97	3.32
4d	0.98	−5.35	−2.03	3.32

[a] Performed in Bu_4NPF_6/CH_2Cl_2 solution, v = 100 mV/s. [b] Calculated by using the empirical equation: HOMO = −(4.44 + $E_{ox}{}^{onset}$). [c] Calculated from E_g and E_{HOMO}. [d] Estimated from the onset of absorption in CH_2Cl_2 ($E_g = 1240/\lambda_{onset}$).

Conclusion

In summary, we report here a new family of ladder-type heteroacenes, the 5,6-disubstituted diindolo[3,2-*b*:4,5-*b*′]thiophenes **4a**−**d**, prepared by an efficient method based on intramolecular cyclization of 3,3′-dibromo-2,2′-biindoles. Single-crystal XRD study demonstrates that tolyl-substituted DIT **4d** adopts a slipped cofacial $\pi-\pi$ packing motif, and propyl-substituted DIT **4b** adopts three types of herringbone packing interlaced patterns. Their crystal structures show that the size of substituents and the molecular dipole moment have effects on the solid-state packing simultaneously, and the S−S interactions enhance the electronic transport between molecules. Coupled with optical properties, the skeleton of diindolo[3,2-*b*:4,5-*b*′]thiophene is more favorable to intermolecular π-stacking in the solid than that of indolo[3,2-

(28) (a) Brédas, J.-L.; Silbey, R.; Boudreaux, D. S.; Chance, R. R. *J. Am. Chem. Soc.* **1983**, *105*, 6555. (b) Pommerehne, J.; Vestweber, H.; Guss, W.; Mark, R. F.; Bässler, H.; Porsch, M.; Daub, J. *Adv. Mater.* **1995**, *7*, 551. (c) Thelakkat, M.; Schmidt, H.-W. *Adv. Mater.* **1998**, *10*, 219.

(29) Meng, H.; Bendikov, M.; Mitchell, G.; Helgeson, R.; Wudl, F.; Bao, Z.; Siegrist, T.; Kloc, C.; Chen, C. H. *Adv. Mater.* **2003**, *15*, 1090.

b]carbazole. **4a**−**d** all exhibit low-lying HOMO energy levels and large band gaps, indicative of good stabilities against oxygen under ambient conditions. Further studies on the applications of these materials to OFETs are in progress in our laboratory.

Experimental Section

1-Propyl-1*H*-indole (1b). To a suspension of KOH (11.20 g, 0.20 mol) in 100 mL of DMF was added indole (4.69 g, 0.04 mol). After the solution was stirred for 1 h, 1-bromopropane (5 mL, 0.055 mol) was added. The reaction mixture was then warmed to 50 °C and stirred overnight. The resulting suspension was poured into water and extracted with CH_2Cl_2. The combined organic layers were washed with water, dried over anhydrous $MgSO_4$, and filtered, and the solvent was removed in vacuo. The crude product was purified by column chromatography (silica gel, eluent: petroleum) to obtain 5.41 g (85%) of **1b** as a yellowish oil: ^{1}H NMR (400 MHz, $CDCl_3$, ppm) δ 7.63 (d, J = 7.84 Hz, 1H), 7.35 (d, J = 8.24 Hz, 1H), 7.19 (t, J = 7.52 Hz, 1H), 7.10−7.07 (m, 2H), 6.48 (d, J = 2.72 Hz, 1H), 4.08 (t, J = 7.08 Hz, 2H), 1.90−1.84 (m, 2H), 0.93 (t, J = 7.40 Hz, 3H); ^{13}C NMR (100 MHz, $CDCl_3$, ppm) δ 136.7, 129.3, 128.4, 121.9, 121.5, 119.8, 110.1, 101.4, 48.4, 24.0, 12.0; EI-MS *m*/*z* (%) 159 (M^+, 100%).

1-Hexyl-1*H*-indole (1c).[20] This compound as a yellow oil was prepared from indole and 1-bromohexane in 87% yield according to the procedure for **1b**: ^{1}H NMR (400 MHz, $CDCl_3$, ppm) δ 7.63 (d, J = 7.72 Hz, 1H), 7.34 (d, J = 8.20 Hz, 1H), 7.19 (t, J = 8.63 Hz, 1H), 7.10−7.08 (m, 2H), 6.48 (s, 1H), 4.09 (t, J = 7.16 Hz, 2H), 1.82 (t, J = 6.59 Hz, 2H), 1.29 (s, 6H), 0.87 (s, 3H); ^{13}C NMR (100 MHz, $CDCl_3$, ppm) δ 136.5, 129.2, 128.2, 121.8, 121.4, 119.6, 109.9, 101.3, 46.7, 31.9, 30.7, 27.1, 23.1, 14.5; EI-MS *m*/*z* (%) 201 (M^+, 100%).

1-p-Tolyl-1*H*-indole (1d). To a suspension of indole (4.69 g, 0.04 mol), K_2CO_3 (22.11 g, 0.16 mol), CuO (6.36 g, 0.08 mol), and 18-crowm-6 (1.06 g, 4 mmol) in 100 mL of DMF was added 4-iodotoluene (13.08 g, 0.06 mol) at reflux with stirring for 32 h. The reaction mixture was filtered through a pad of silica gel, and the solvent of the filtrate was removed in vacuo. The crude product was purified by column chromatography (silica gel, eluent: petroleum/ethyl acetate = 4:1) to obtain 6.55 g (79%) of **1d** as a yellowish oil: ^{1}H NMR (400 MHz, $CDCl_3$, ppm) δ 7.69 (d, J = 7.76 Hz, 1H), 7.54 (d, J = 8.14 Hz, 1H), 7.40 (d, J = 8.05 Hz, 2H), 7.32−7.31 (m, 3H), 7.23−7.14 (m, 2H), 6.67 (d, J = 3.04 Hz, 1H), 2.44 (s, 3H); ^{13}C NMR (75 MHz, $CDCl_3$, ppm) δ 136.1, 135.1, 134.8, 129.0, 128.1, 126.9, 123.1, 121.1, 119.9, 119.1, 109.4, 102.1, 19.9; EI-MS *m*/*z* (%) 207 (M^+, 100%).

1,1′-Dipropyl-1*H*,1′*H*-2,2′-biindole (2b). To a stirred solution of **1b** (4.61 g, 29 mmol) in 150 mL of diethyl ether at room temperature was added dropwise a solution of *n*-BuLi (14.5 mL, 36 mmol) under argon atmosphere over 20 min. The reaction mixture was heated at reflux with stirring under an inert gas atmosphere for 4 h and then allowed to cool to room temperature. Anhydrous copper(II) chloride (3.9 g, 29 mmol) was then added in three portions and the mixture was again heated under reflux for 2 h. After being allowed to cool to room temperature, the mixture was left to stand for 1 h before being poured into ice/water. The dirty brown-green precipitate was filtered off, the organic layer was separated, and the aqueous phase was extracted twice with diethyl ether. The precipitate was washed twice with CH_2Cl_2 and the filtrate combined with the ether phase. The combined organic phases were dried with anhydrous $MgSO_4$ then concentrated, and the residue was purified by column chromatography (silica gel, eluent: petroleum) to obtain 3.16 g (69%) of **2b** as a white solid: ^{1}H NMR (400 MHz, $CDCl_3$, ppm) δ 7.68 (d, J = 7.80 Hz, 2H), 7.41 (d, J = 8.20 Hz, 2H), 7.28 (dd, J = 15.21 Hz, J = 6.60 Hz, 2H), 7.15 (t, J = 7.40 Hz, 2H), 6.61 (s, 2H), 4.02 (t, J = 7.54 Hz, 4H), 1.75−1.65 (m, 4H), 0.78 (t, J = 7.40 Hz, 6H); ^{13}C NMR (75 MHz, $CDCl_3$, ppm) δ 137.1, 131.4, 128.0, 122.2, 121.1, 120.0, 110.4, 104.8, 45.9, 23.5, 11.5; EI-MS *m*/*z* (%) 316 (M^+, 100%). Anal. Calcd for $C_{22}H_{24}N_2$: C, 83.50; H, 7.64; N, 8.85. Found: C, 83.49; H, 7.67; N, 8.75.

3,3′-Dibromo-1,1′-dipropyl-1*H*,1′*H*-2,2′-biindole (3b). The 2,2′-biindole **2b** (2.18 g, 6.9 mmol) was dissolved in 50 mL of DMF and a solution of bromine (0.8 mL, 15.6 mmol) in 20 mL of DMF was added dropwise with stirring at room temperature. The mixture was stirred for 15 min and then poured into 100 mL of ice/water containing ammonia (0.5%) and sodium metabisulfite (0.1%), then extracted with CH_2Cl_2. The organic layer was washed with water, dried over anhydrous $MgSO_4$, and filtered, then the solvent was removed in vacuo. The crude product was purified by column chromatography (silica gel, eluent: petroleum) to obtain 3.07 g (94%) of **3b** as a white solid: ^{1}H NMR (400 MHz, $CDCl_3$, ppm) δ 7.69 (d, J = 7.93 Hz, 2H), 7.44 (d, J = 8.27 Hz, 2H), 7.35 (t, J = 7.58 Hz, 2H), 7.26 (t, J = 6.92 Hz, 2H), 4.09−4.02 (m, 2H), 3.81−3.74 (m, 2H), 1.73−1.63 (m, 4H), 0.78 (t, J = 7.43 Hz, 6H); ^{13}C NMR (100 MHz, $CDCl_3$, ppm) δ 136.7, 127.4, 127.3, 123.8, 120.7, 120.2, 110.7, 95.8, 47.1, 23.4, 11.6; EI-MS *m*/*z* (%) 474 (M^+, 100%). Anal. Calcd for $C_{22}H_{22}Br_2N_2$: C, 55.72; H, 4.68; N, 5.91. Found: C, 55.93; H, 4.71; N, 5.84.

5,6-Dimethyldiindolo[3,2-*b*:4,5-*b*′]thiophene (4a). To a solution of **3a** (2.02 g, 4.3 mmol) in 150 mL of diethyl ether at −78 °C was added dropwise a solution of *n*-BuLi (3.8 mL, 9.5 mmol) under argon. After the solution was stirred for 1 h at −78 °C, $(C_6H_5SO_2)_2S$ (1.66 g, 5.3 mmol) was added. The reaction mixture was then warmed to room temperature and stirred overnight. Water (100 mL) was added, and the ether layer was washed with water. The combined aqueous layers were washed with diethyl ether, and the separated organic layers were dried over anhydrous $MgSO_4$ and filtered. The solvent was removed in vacuo. The crude product was purified with column chromatography (silica gel, eluent: petroleum) to obtain 636 mg (51%) of **4a** as a light yellow solid: ^{1}H NMR (400 MHz, $CDCl_3$, ppm) δ 7.76 (d, J = 7.76 Hz, 2H), 7.45 (d, J = 8.24 Hz, 2H), 7.32 (t, J = 7.50 Hz, 2H), 7.21 (t, J = 7.42 Hz, 2H), 4.18 (s, 6H); ^{13}C NMR (75 MHz, $CDCl_3$, ppm) δ 141.7, 130.9, 123.0, 122.5, 119.6, 118.4, 109.9, 33.8; EI-MS *m*/*z* (%) 290 (M^+, 100%). Anal. Calcd for $C_{18}H_{14}N_2S$: C, 74.45; H, 4.86; N, 9.65. Found: C, 74.11; H, 5.11; N, 9.31.

5,6-Dipropyldiindolo[3,2-*b*:4,5-*b*′]thiophene (4b). This compound as a white solid was prepared from **3b** in 53% yield according to the procedure for **4a**: ^{1}H NMR (400 MHz, $CDCl_3$, ppm) δ 7.74 (d, J = 7.84 Hz, 2H), 7.44 (d, J = 8.28 Hz, 2H), 7.29 (t, J = 7.44 Hz, 2H), 7.21−7.17 (m, 2H), 4.45 (t, J = 7.78 Hz, 4H), 2.00−1.91 (m, 4H), 1.00 (t, J = 7.40 Hz, 6H); ^{13}C NMR (75 MHz, $CDCl_3$, ppm) δ 141.3, 130.3, 123.2, 122.5, 120.1, 119.7, 118.4, 110.3, 48.0, 24.1, 11.5; EI-MS *m*/*z* (%) 346 (M^+, 100%). Anal. Calcd for $C_{22}H_{22}N_2S$: C, 76.26; H, 6.40; N, 8.08. Found: C, 75.84; H, 6.54; N, 7.95.

Acknowledgment. The present research was financially supported by the National Natural Science Foundation (60671047, 50673093, 60736004, 20573115, 20721061), the Major State Basic Research Development Program (2006CB806203, 2006-CB932103), and the Chinese Academy of Sciences.

Supporting Information Available: General experimental procedures and ^{1}H and ^{13}C spectra for all new compounds, as well as crystallographic data for **4b** and **4d** presented in CIF format. This material is available free of charge via the Internet at http://pubs.acs.org.

JO800622Y